IV International Conference on Simulation for Additive Manufacturing
Sim-AM 2023
E. Rank and S. Kollmannsberger (Eds)

SIMULATION BASED PROCESS OPTIMIZATION TOWARDS HOMOGENEOUS TI6AL4V COMPONENTS

TIM P.A. KOENIS*, MARIA L. MONTERO-SISTIAGA*, MARC J. DE SMIT* AND EMIEL AMSTERDAM*

* Royal Netherlands Aerospace Centre (NLR)
Anthony Fokkerweg 2, 1059 CM Amsterdam, Netherlands
e-mail: tim.koenis@nlr.nl, web page: http://www.nlr.org

Key words: numerical simulations, Additive manufacturing, process optimization, Ti6Al4V, overheating

Abstract. In this study, macro-scale thermal simulation of the laser powder bed fusion (L-PBF) process is employed to predict and limit geometry-induced overheating of complex Ti6Al4V components. First, the overheating effect is reproduced in tensile specimens. Overheating is found to increase the local oxygen content by almost 80% and lower the elongation at break by over 70% in overheated regions. By employing macro-scale thermal simulations, an automated routine is developed to efficiently optimize the L-PBF process to prevent local overheating. Variable interlayer wait times are numerically optimized to allow cooling of the material without adding manufacturing time where this is not required. In this way, local overheating can successfully be prevented resulting in a more homogeneous temperature distribution during the L-PBF process. This method was found to fully restore the mechanical properties in geometries prone to overheating, resulting in more homogeneous and predictable Ti6Al4V components.

1 INTRODUCTION

Additive manufacturing is a manufacturing process which is gaining popularity within the aerospace sector thanks to the possibilities offered by this technology to manufacture highly optimized, complex and lightweight structures. However, certification of L-PBF critical parts remains difficult in the aerospace sector, partly due to large variations in mechanical properties and fatigue behaviour. Complex L-PBF part geometries can severely influence the local microstructure and porosity level resulting in different mechanical and fatigue properties throughout L-PBF components [1–3]. In Ti6Al4V, heat accumulation during the L-PBF process is found to significantly increase the dissolution of oxygen, creating locally embrittled material [4]. These geometry introduced effects could result in the need of excessive print iterations or even go unnoticed until the component is extensively tested. By identifying the overheated regions early in the component development, adequate preventive measures can be taken before

production to prevent additional work and costs.

The geometry induced overheating generally occurs in features with large scan areas with respect to underlying material conducting heat to the baseplate. This heat accumulation effect is often observed to develop over multiple L-PBF layers depending on the printed geometry. This makes it ideal to predict and identify these regions by relatively fast part scale process simulation methods. To speed up simulation time, these models generally simulate the L-PBF process using multiple layers per time increment. Even though melt-pool behaviour is not captured with this method, interlayer temperatures and heat accumulation can be predicted [5].

In the present work, an iterative numerical method was developed to optimize the L-PBF process of Ti6Al4V to prevent geometry induced heat accumulation. The numerical modelling approach employed fast, low fidelity finite element models (FEM) using ABAQUS to predict overheating. As the simulation methods are to be used during the preparation of the print, fast simulations are desired over the more impractical computationally heavy models. In this study, the process was optimized by adjusting the interlayer time (ILT), making sure the machine waits long enough for the material to cool down, but no longer. First, the overheating effect was replicated in a predictable setting using conical geometries in vertically printed tensile specimens. These specimens were manufactured both with the original process parameters, as well as using the numerically optimized process. Additionally, regular tensile specimens without the conical geometry have been manufactured with the same orientation and print parameters as reference. The tensile specimens were mechanically tested and analysed on oxygen content to observe the effect of the heat accumulation and the variable ILT optimization. Furthermore, the simulation-based process optimization strategy has been tested on a more general topology optimized aerospace bracket.

2 METHODS

In this study, an SLM 280 L-PBF machine was used to manufacture Ti6Al4V specimens. The components were manufactured with a laser power of 270 W, a scan velocity of 1000 mm/s, a hatch distance of 0.13 mm and a layer thickness of 50 µm. A Ti6Al4V grade 23 powder was used supplied by LPW with a particle size distribution between 20 and 63 µm. The process was performed under a constant argon gas flow with less than 100 ppm oxygen content and with baseplate preheating of approximately 150 °C.

In this study, the overheating in Ti6Al4V components was investigated which is an effect that accumulates over multiple layers of the L-PBF process. Therefore, a part scale thermal simulation is well suited for the prediction and eventual prevention of this overheating. Figure 1 (a) displays the thermal model schematically. Per time increment, a new meta layer is activated consisting of 10 L-PBF layers. The duration of each time increment is directly taken from the build files containing the scan vector data. Heat is applied to these layers according to the scan vector data and absorptivity of the material of 0.45. Convective and radiation heat loss is modelled on the top surface with a convection coefficient of 5 $\frac{W}{m^2K}$ and an emissivity of 0.25. Heat exchange with the heating element below the baseplate is modelled at the bottom of the baseplate with a heat transfer coefficient of 60 $\frac{W}{m^2K}$. The thermal conductivity, specific heat and material density are modelled temperature dependent based on Chiumenti et al [6].

To replicate the effects of heat accumulation systematically, tensile specimens with an

integrated conical structure have been designed as shown in Figure 1 (b). The numerical model was employed to ensure the cone height and angle (θ) result in interlayer temperatures over 350 °C throughout the gauge section. This temperature should result in significant overheating effects in the manufactured specimens [4, 7]. From the numerical simulations, it was observed that only three overheating specimens can be manufactured per build with an cone angle θ of 30° to guarantee that the interlayer temperature remains above the threshold. After manufacturing, the specimens are stress relieved for 2 hours at 780 °C and subsequently removed from the baseplate. The gauge section is machined down to a diameter of 5 mm. The reference specimens manufactured without conical section were heat treated and machined in similar fashion. From both types of specimens, an overheated and a reference specimen , three 120 mg slices were taken to determine the oxygen content. The inert gas fusion (IGF) method was carried out by Oerlikon Metco.

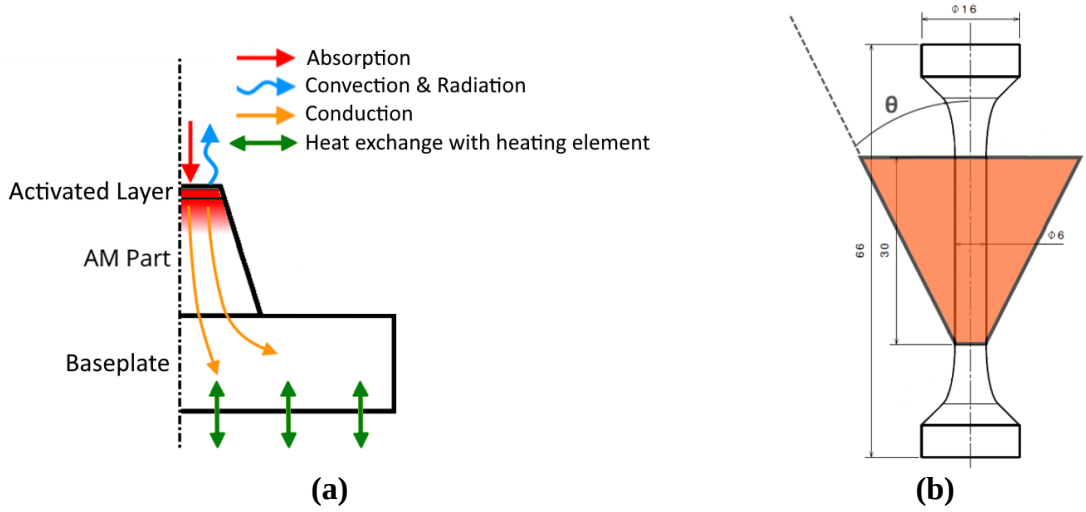

Figure 1: (a) schematic overview of the part scale thermal model built in ABAQUS and (b) the design of the tensile specimens with integrated top-down cone geometry to induce sufficient overheating.

To investigate the numerical process optimization approach, the same tensile specimens with conical section were used. An effective way to counteract overheating was found to be the introduction of additional interlayer time (ILT) [4, 8]. In multiple studies, the introduction of a longer, fixed ILT showed a significant reduction in overheating effects. However, in these studies, the fixed ILT introduced wait times also in layers where this is not required. To not introduce extremely long manufacturing times, the ILT can be varied per layer and optimized to ensure that overheating is avoided without introducing too much additional manufacturing time. For this ILT optimization, low fidelity and fast part scale numerical simulations have been employed. A thermal model of the overheating tensile specimen was built as shown in Figure 2 (a), including the baseplate and support structures. The thermal model employs a mesh of 2x2x2 mm hexahedral linear elements. Furthermore, only one specimen was included to further limit computational time, resulting in a total simulation time of less than 5 minutes when run on four CPUs.

Figure 2 (b) displays the iteration schematic of the ILT optimization. First, the component is split into control regions as shown in Figure 2 (a). These regions determine the resolution of

the ILT variation, since the interlayer temperature is extracted and interlayer wait times are altered per region. The first iteration is simulated using the minimum ILT, which corresponds to the total time required for the deposition of a new powder layer. As per the schematic of Figure 2 (b), the regional temperatures are extracted from the result of the thermal simulation and compared with the set threshold temperature (T_{set}) of 300 °C. If the temperatures are above this threshold, the ILT should be increased. If the temperatures are below the threshold and the ILT is longer than the minimum, the ILT should be lowered. After these adjustments are made, the simulation is run again, resulting in different interlayer temperatures. This is repeated until all interlayer temperatures are just below the threshold temperature or already use the minimum allowed ILT.

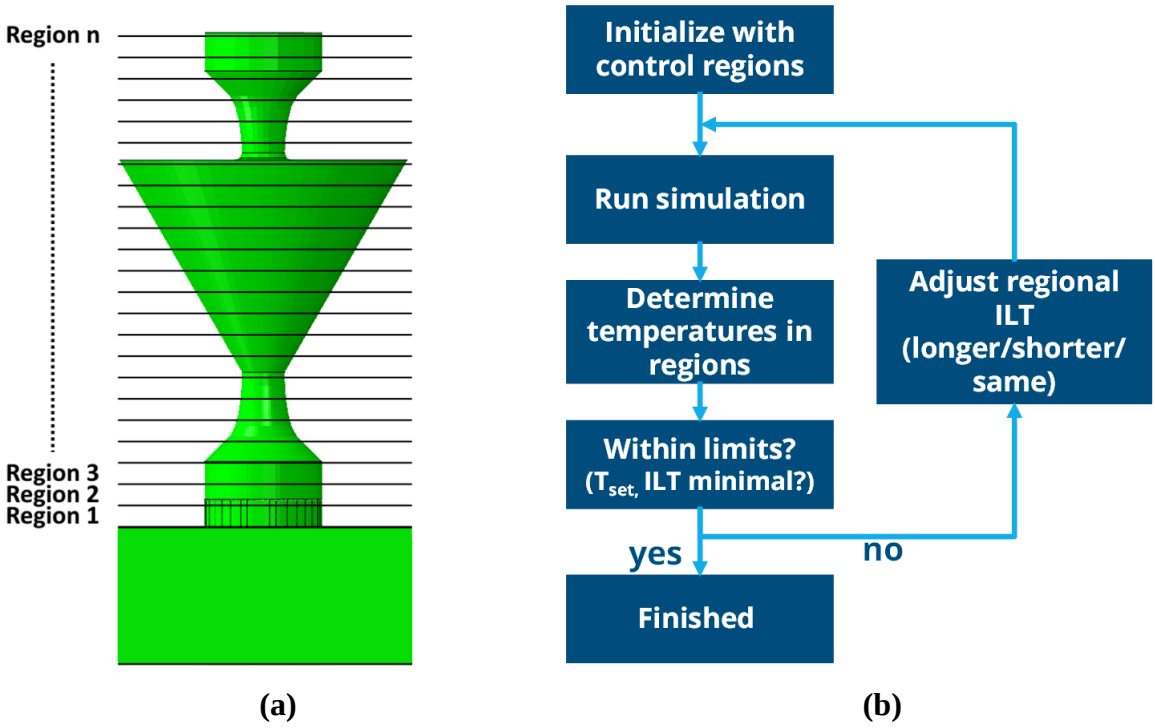

Figure 2: (a) numerical model of the tensile specimen with integrated cone section divided in n control regions and (b) a schematic overview of the optimization process optimizing the ILT per control region

From the ILT optimization, the optimal wait time per control region was obtained. However, currently, the L-PBF machine can only use a single wait time throughout the print. To incorporate the optimized variable wait times a "ghost part" approach has been used. The optimized wait times were translated into a circular area that requires a time to print equal to the optimal wait time minus the time required for recoating. These areas were extruded to cylinders equal to the height of the corresponding control region. By stacking the cylinders of each control region a 3-dimensional shape was defined that introduces the optimal wait time in each layer. By scanning this part with 0 W, the "ghost part" was not physically printed, but the wait time is included. Similar to the overheated specimens, the specimens manufactured with ghost part have been stress relieved and machined to obtain the test specimen geometry.

3 RESULTS AND DISCUSSION

During the manufacturing of the specimens with integrated conical geometry, significant overheating effects were visible illustrated by the afterglow observed in Figure 3 (a). After manufacturing, the overheated conical section showed a slightly different colour and surface texture compared to the rest of the specimen Figure 3 (b). After machining, all specimens were tested with a smooth surface finish. In total, 6 overheated specimens were manufactured in two prints and tested in tensile.

(a) **(b)** **(c)**

Figure 3: (a) an image taken during the manufacturing of the overheated specimen, showing glowing of an area which was just scanned, (b) the complete specimen geometry and (c) the specimen after post-processing

Figure 4 displays the result of the numerical ILT optimization for a print containing three tensile specimens with integrated cone geometry. Figure 4 (a) displays the normalized interlayer temperature over the control regions for multiple iterations during the optimization. After 7 iterations, it is observed that all interlayer temperature profiles were below the threshold. However, in some regions, the wait time was too long, resulting in lower interlayer temperatures than required. Therefore some further iterations were performed until all interlayer temperatures are equal or below the threshold temperature and all interlayer times are as short as possible. In total, 9 iterations were required for this print, resulting in a total optimization time of just over 40 minutes. To verify the optimized wait time and subsequently defined ghost part, a simulation was performed with the scan vector data of the print incorporating the ghost part with three overheating specimens. Figure 4 (b) displays the normalized interlayer temperatures comparing the original process and the optimized process. By incorporating the optimized ghost part, it was observed that throughout the specimen no overheating occurs.

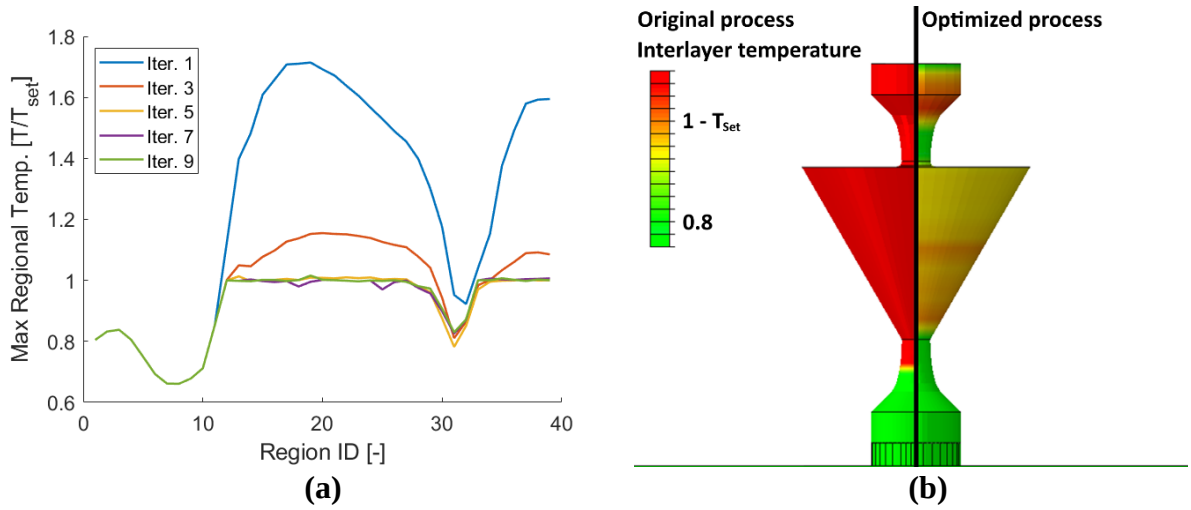

Figure 4: (a) results of subsequent iterations of the ILT optimization loop and (b) a comparisson in maximum temperature in the original process and the optimized process

Figure 5 (a) displays the layout of the print containing the optimized ghost part geometry. Two prints have been manufactured resulting in a total of 6 specimens with integrated cone using optimized ILT. To validate the wait times introduced by the ghost part, the scan time per layer was extracted from the machine log and compared with the simulated events obtained from the optimization. Figure 5 (b) shows that there is only a slight difference between the actual and the predicted scan time, confirming that the ghost part implementation worked as intended. It should be noted that for the prints with three specimens with integrated cone, the optimized ILT introduced an additional 66% of manufacturing time.

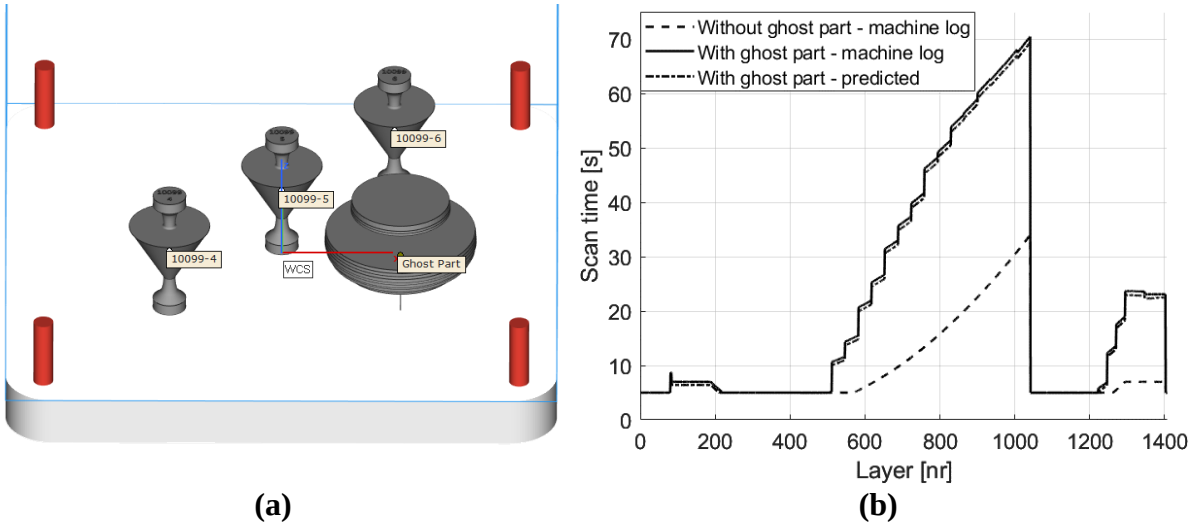

Figure 5: (a) print layout of the specimens with integrated cone combined with the optimized ghost part geometry and (b) comparison of the actual and the predicted scan time per layer.

Figure 6 displays the quasi-static tensile test results for the ultimate tensile strength (UTS), yield strength and failure strain comparing the regular specimens with the overheated geometry

specimens as well as the specimens with optimized ILT. The overheated specimens show a slight increase in UTS and yield strength, however also an extreme reduction in failure strain of >70%. Oxygen testing showed that the integrated cone specimens contained 1600 ± 100 ppm of oxygen in the overheated conical section compared to 900 ± 100 ppm of oxygen observed in the regular specimens. The oxygen content in the used powder was 700 ppm. This shows that similar to Pauzon et al., oxygen content was almost doubled due to the change in geometry [4].

The integrated cone specimens that have been manufactured with optimized ILT showed a significant improvement of the elongation at break compared to the same geometry without optimized ILT. Furthermore, the specimens with optimized ILT showed the same UTS and yield strength as the regular specimens.

It is observed that when the ILT optimization is used in a geometry prone to overheating, the mechanical properties are almost fully restored and comparable to the regular specimens. This shows that the simulation-based process optimization method is successful in the prevention of significant overheating in Ti6Al4V and results in more predictable mechanical properties. It should be noted that this method comes at a significant cost in machine time. To limit this impact while maintaining a predictable and homogeneous process, more process parameters could be included in the optimization. By scaling laser power in overheated areas overheating could be reduced without significant impact on the manufacturing time [7]. However, care must be taken to keep the process stable enough to produce fully dense components.

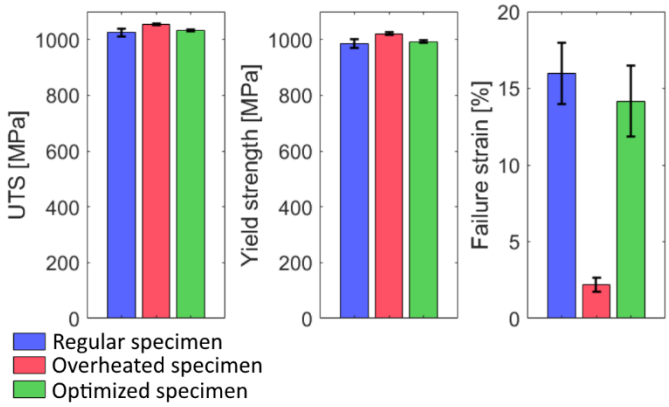

Figure 6: Quasi-static tensile test results of ultimate tensile strength (UTS), yield strength and failure strain for regular specimens, overheated geometry specimens and overheated geometry specimens with optimized interlayer times.

4 USE-CASE

The developed numerical optimization method has been applied to a more complex geometry to investigate its potential. Figure 7 (a) shows a Ti6Al4V actuator fitting that has been optimized by structural topology optimization and manufactured by L-PBF in Ti6Al4V. Part scale thermal simulation showed that significant overheating occurs in certain regions of the component. The simulation-based process optimization has been applied to prevent this local overheating of the material. Due to the larger and more complex geometry, the numerical optimization took 7 hours to complete. Figure 7 (b) displays the numerically determined interlayer temperatures comparing the original process with the optimized ILT process. The

optimized process shows a significant improvement in the thermal homogeneity during manufacturing, fully negating local overheating. Furthermore, in contrast with the tensile specimen with cone geometry, the ILT optimization only added 10% of additional manufacturing time for this complex bracket.

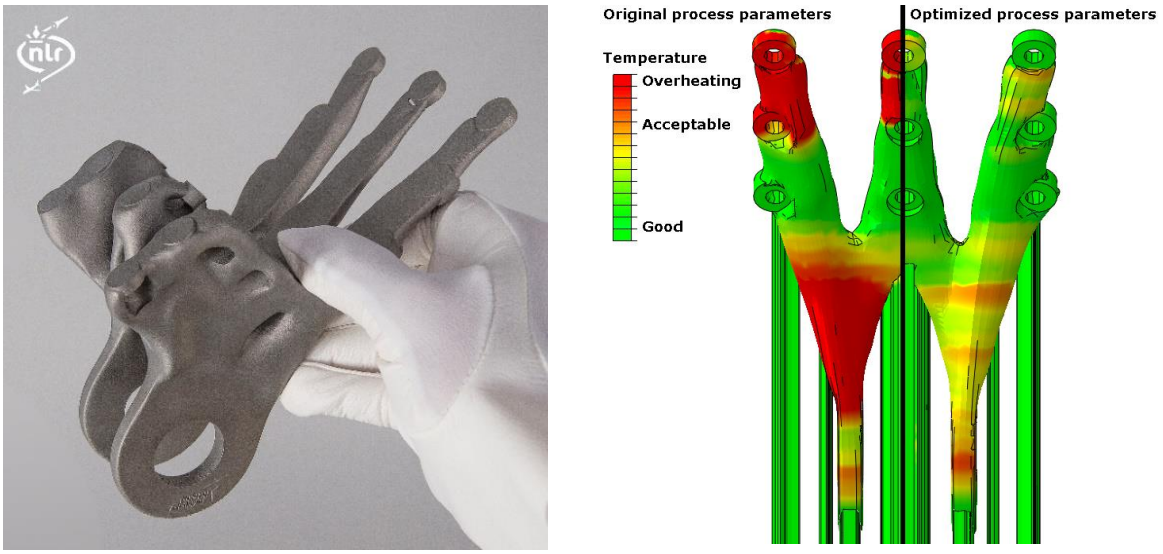

Figure 7: (a) a topology optimized actuator fitting manufactured by L-PBF and (b) comparison of the part scale numerical results with the original process parameters and optimized process parameters.

5 CONCLUSIONS

In this work, it was observed that the geometry of the component can significantly influence the L-PBF process, resulting in significantly different mechanical properties. Specifically in Ti6Al4V, geometry driven heat accumulation over multiple layers can strongly increase oxygen pickup and reduce the failure strain. This heat accumulation can be predicted by part scale thermal simulation, allowing for the implementation of counter measures.

Simulation-based process optimization was found to be very successful in preventing overheating in Ti6Al4V tensile specimens by optimizing a variable interlayer wait time. This method resulted in fully restored mechanical properties in geometries that would otherwise overheat. When applying this method to representative complex Ti6Al4V L-PBF components, the additional manufacturing time increases to some extent, however the component can be manufactured with more homogeneous and predictable properties. As this would result in better certifiability in aerospace, these kinds of process optimization methods could become crucial for further implementation of AM for flight critical components.

6 ACKNOWLEDGEMENTS

This work has been funded by the NLR Metal Additive Manufacturing II programme, an international Public Private Partnership. The authors would like to thank Ludo Bautmans and Alper Evirgen for the IGF test and the fruitful discussions.

REFERENCES

[1] P. Barriobero-Vila *et al.*, 'Mapping the geometry of Ti-6Al-4V: From martensite decomposition to localized spheroidization during selective laser melting', *Scripta Materialia*, vol. 182, pp. 48–52, Jun. 2020, doi: 10.1016/j.scriptamat.2020.02.043.

[2] J. Munk, E. Breitbarth, T. Siemer, N. Pirch, and C. Häfner, 'Geometry Effect on Microstructure and Mechanical Properties in Laser Powder Bed Fusion of Ti-6Al-4V', *Metals*, vol. 12, no. 3, p. 482, Mar. 2022, doi: 10.3390/met12030482.

[3] Y. Cai, T. Lu, G. Ma, W. Li, Y. Pan, and H. Ding, 'Effects of geometrical characteristics on defect distributions in alloy components produced by selective laser melting', *China Foundry*, vol. 18, no. 4, pp. 369–378, Jul. 2021, doi: 10.1007/s41230-021-1048-0.

[4] C. Pauzon, K. Dietrich, P. Forêt, E. Hryha, and G. Witt, 'Mitigating oxygen pick-up during laser powder bed fusion of Ti-6Al-4V by limiting heat accumulation', *Materials Letters*, vol. 288, p. 129365, Apr. 2021, doi: 10.1016/j.matlet.2021.129365.

[5] M. Bayat, W. Dong, J. Thorborg, A. C. To, and J. H. Hattel, 'A review of multi-scale and multi-physics simulations of metal additive manufacturing processes with focus on modeling strategies', *Additive Manufacturing*, vol. 47, p. 102278, Nov. 2021, doi: 10.1016/j.addma.2021.102278.

[6] M. Chiumenti *et al.*, 'Numerical modelling and experimental validation in Selective Laser Melting', *Additive Manufacturing*, vol. 18, pp. 171–185, Dec. 2017, doi: 10.1016/j.addma.2017.09.002.

[7] A. Riensche *et al.*, 'Feedforward control of thermal history in laser powder bed fusion: Toward physics-based optimization of processing parameters', *Materials & Design*, vol. 224, p. 111351, Dec. 2022, doi: 10.1016/j.matdes.2022.111351.

[8] G. Mohr, S. J. Altenburg, and K. Hilgenberg, 'Effects of inter layer time and build height on resulting properties of 316L stainless steel processed by laser powder bed fusion', *Additive Manufacturing*, vol. 32, p. 101080, Mar. 2020, doi: 10.1016/j.addma.2020.101080.